Original Article

# The Possible Protective Role of Moringa Oleifera on High Fat Diet Induced Injury on the Renal Cortex of Adult Male Rats. Histological and Biochemical study

*Asmaa Abd El Aziz, Hanan A. Saleh, Gehan Abd El Khalek Ibrahim and Faika Hassan El Ebiary*

*Department of Histology, Faculty of Medicine, Ain Shams University, Cairo, Egypt*

## ABSTRACT

**Introduction:** Consumption of high fat diet (HFD) is common worldwide which may cause several complications including chronic kidney disease. Moringa oleifera (MO) is a well-known herb that has been widely used for its numerous pharmacological properties.

**Aim of the Work:** To evaluate the possible protective role of MO on HFD induced renal cortex injury in adult male rats.

**Material and Method:** Three groups of thirty rats weighing 180–200 g, aged 8 week were used. Group I: control, group II: HFD and group III: HFD and MO aqueous extract (1000 mg/kg/day). After four weeks, body weights were recorded, blood samples were taken to determine level of fasting blood glucose, lipid profile, kidney function tests and kidneys were processed for light and electron microscopic examination. Immunohistochemical, histomorphometric and statistical studies were performed.

**Results:** Group II (HFD) rats revealed significantly increased mean body weight, mean level of fasting blood glucose, triglycerides, cholesterol, LDL, urea, and creatinine in comparison to group I. Microscopic examination showed focal changes of the renal cortex. The glomerular capillaries showed thickened glomerular basement membrane, focal adhesions between the capillary tuft and Bowman's capsule, apparent increased number of intraglomerular mesangial cells, fusion of podocytes processes with reduction of sub-podocytic space. The renal tubules were disorganized and the lumina contained acidophilic casts and exfoliated cells. PCTs showed loss of brush borders and numerous disorganized small sized mitochondria. In the interstitium, mononuclear cellular infiltration, increased collagen deposition and positive α-SMA reaction were detected. However, group III rats showed preserved renal cortical structure as well as preserved biochemical profile and mean body weight.

**Conclusions:** Supplementation with MO ameliorated the HFD induced body weight gain and disturbed biochemical profile with preservation of most of the structure of the renal cortex.

**Received:** 11 March 2025, **Accepted:** 08 April 2025

**Key Words:** α-SMA, high fat diet, kidney cortex, moringa oleifera, rat.

**Corresponding Author:** Asmaa Abd El Aziz Esmael, MD, Department of Histology, Faculty of Medicine, Ain Shams University, Cairo, Egypt, **Tel.**: +20 10 9996 7474, **E-mail:** asmaa_abdelaziz@med.asu.edu.eg

**ISSN:** 1110-0559, Vol. 48, No. 2

## INTRODUCTION

High fat diet (HFD) denotes to the feeding of foods that contain at least 35% of the total calories from fat[1]. Due to lifestyle modifications and appealing flavor, HFD has gained widespread acceptance and popularity among an increasing number of individuals. However, it induces the pathogenesis of metabolic disorders as obesity, hyperglycemia, and cardiovascular disorders[2].

Metabolic syndrome is known as a collection of clinical, physiological, biochemical and metabolic features. Increased visceral obesity, hypertension, insulin resistance as well as dyslipidemia are its hallmarks. Being a predisposing factor for both type 2 diabetes mellitus and cardiovascular disorders, metabolic syndrome is a global issue that contributes to rising death rates[3]. People who have metabolic syndrome are more likely to get chronic renal disease which increases cardiovascular morbidity as well as mortality[4]. Potential mechanisms that might link metabolic syndrome with chronic renal disorders include endothelial dysfunction, insulin resistance, inflammation, mitochondrial dysfunction, and oxidative stress[5].

Moringa oleifera (MO) is a well-known highly nutritional herb that has been widely used in folk medicine. It has been given the name "the Miracle Tree" due to its numerous pharmacological potentials[6]. The reported pharmacological properties of MO include antioxidant, anti-cancer, anti-diabetic, anti-inflammatory, anti-allergic, anti-ulcer and anti-pyretic effects. Moringa oleifera is also known by its obesity management effect[7].

Previous studies reported the harmful consequences of the HFD on the different organs of the body including the kidney. However, there is insufficient data describing

*DOI: 10.21608/ejh.2025.367367.2227*

the possible protective role of the natural herbs against the effect of the HFD on the renal tissue.

The purpose of this study was to assess the potential protective role of moringa oleifera on the deleterious effect of High fat diet on the renal cortex of adult male rats.

## MATERIALS AND METHODS

### *Experimental animals*

Thirty adult male albino Wistar rats weighing 180–200 g and 8 weeks of age were utilized in this study. The animals were purchased and raised in Ain Shams Research Institute, Faculty of Medicine. For the period of the experiment, all animals were placed in hygienic plastic cages with mesh wire covers, five rats in each cage, gained unrestricted access to food and water, and maintained at the ideal conditions of light, humidity (40 ± 5%), and temperature (23 ± 2$^{o}$ C).

All animal procedures were authorized by the Faculty of Medicine Ain Shams University Research Ethics Committee and carried out in compliance with the general rules for the care and use of laboratory animals. (FMASU MD 228/2021).

### *Dietary formula preparations*

High fat diet was prepared at MASRI (Faculty of Medicine Ain Shams University Research Institute). It contained fat (57.4%), carbohydrate (24.69%) as well as protein (14.37%) in 100 grams of dry food, with a total caloric value of 672.72 kcal/100 grams dry food, while the standard diet was composed of fat (5.56%), carbohydrate (67.4%) and protein (23.47%) in 100 grams of dry food, with a total caloric value of 413.6 kcal/100 grams dry food[8].

### *Moringa oleifera aqueous extract*

It was purchased from the National Research Centre, Giza, Egypt in the form of pre-equipped ready to use bottles. The experimental animals received a regular dosage of the extract (1000 mg/kg/day)[9].

### *Experimental design*

Rats were acclimatized for seven days before being divided into three groups randomly and were fed their specified diets for four weeks as follows:

**Group I:** served as control group and included ten animals which were further subdivided into two equal subgroups: Subgroup Ia: rats were given the standard chew diet and subgroup Ib: rats were given the standard diet in addition to MO aqueous extract via intragastric tube at a dose of 1000 mg/kg/day.

**Group II (HFD group):** Included ten rats that were fed HFD.

**Group III (HFD and MO):** Included ten rats that were fed HFD in addition to MO aqueous extract via intragastric tube at a dose of 1000 mg/kg/day.

After four weeks, all animals were anesthetized by ether inhalation, blood samples had been taken from their tail veins, and then rats were sacrificed. The kidney specimens were carefully dissected from adherent soft tissues for further processing.

### *Methods*

#### Weight measurements

The weight of each rat from each group was measured at the start of experiment and just before the time of sacrifice.

#### Biochemical studies

Following an overnight fast, blood samples were taken in the morning of the last day of the experiment just before sacrifice to measure the level of fasting blood glucose, total cholesterol (CH), serum triglyceride (TG), serum low-density lipoproteins (LDL), serum high-density lipoproteins (HDL), blood urea and blood creatinine level.

#### Light microscopic studies

Right kidney specimens were fixed in 10% neutral buffered formaldehyde for a week. After that, specimens were dehydrated in increasing alcohol grades, cleared in xylene and embedded in paraffin. Serial paraffin sections were cut at 5µm thickness and stained with the following histological as well as immuno-histochemical stains. They included Haematoxylin and Eosin (H&E), Masson's trichrome stain, Periodic Acid Schiff reaction (PAS)[10].

Immuno-histochemical staining was performed using a polyclonal rabbit anti-rat α-SMA primary antibody and Goat anti-rabbit secondary antibody for detection of myofibroblast (#A7248-Abclonal Tecnology®). Antibodies were incubated overnight at 4°C. The cytoplasm of the myofibroblast and vascular smooth muscle showed variable degrees of brown cytoplasmic staining, indicating positive immunoreactivity. Negative control sections were processed by replacing the primary antibody by phosphate buffer saline, while positive control immunohistochemistry of paraffin embedded rat colon tissue showed brown cytoplasmic reaction in the smooth muscle of the colon[10].

#### Transmission electron microscopic study

Very small specimens (1-2mm$^{3}$) were taken from the cortex of left kidney in all animal groups and were processed for semithin and ultrastructural examination[10]. The grids were examined using the transmission electron microscope (TEM) JEM 1200 EXII (JEOL, Tokyo, Japan) in Faculty of Agriculture, Cairo University Research Park (CURP).

### *Histomorphometric measurements*

The following morphometric parameters were measured: The area percentage of collagen fibers in Masson's trichrome stained sections (X 20), and the area percentage of positive α-SMA reaction (X 20). All measurements were done in five distinct slides by examination of five non-overlapping fields for each slide.

The measurements were performed by image analysis at Ain Shams University -Faculty of Medicine- Department of Histology using Leica Q win software.

### *Statistical analysis*

A statistical analysis was performed on the weight, biochemical, and histomorphometric measurements that were acquired. The SPSS statistical software, version 21 (IBM Inc., Chicago, Illinois, USA), was used to determine the mean value and the standard deviation (SD) for each group. Data were statistically analyzed using one way analysis of variance (ANOVA) with post-hoc test for comparison between means. Values were presented as mean ± SD. The data significance was assessed by probability of chance (*P- value*) where; $p<0.05$ was considered significant and $p>0.05$ was considered non-significant.

## RESULTS

All rats of the different groups remained alive throughout the experiment.

### *Body weight*

Statistically, there was a non-significant change between the control subgroups. There was a significant increase in the mean weight of the body of animals of HFD group (II) compared to that of control group (I). However, the mean weight of the body of animals of groups III (HFD and MO) was significantly decreased in comparison with group II and it was non-significantly different in comparison with that of group I. (Table 1).

### *Biochemical results*

The control group revealed that there was a non-significant change in the measured parameters between its subgroups. On the other hand, in group II (HFD) all biochemical parameters showed a significant difference in comparison with the control group. Moreover, in group III (HFD and MO), there was a significant improvement in the biochemical parameters in comparison with group II.

In group II (HFD), the mean blood glucose level, TG, CH, and LDL were significantly increased as compared to that of group I. Meanwhile, the mean level of the same parameters of group III animals (HFD and MO) showed a significant reduction in comparison with HFD group (II) and a non-significant difference in comparison with group I. As regards the mean HDL blood level, there was a significant reduction in the animals of group II in comparison with group I. In addition, group III had significantly increased levels of HDL as compared to group II as well as a non-significant change as compared to group I (Table 1).

Animals in group II (HFD) had significantly higher mean blood levels of creatinine and urea than those in group I. Moreover, the mean blood urea level of animals of groups III (HFD and MO) was significantly lower than those in HFD group and significantly higher as compared to control group. The mean blood creatinine level of animals of group III showed a significant reduction in comparison to group II and a non-significant change in comparison to group I (Table 1).

### *Histological findings*

Control subgroups (Ia and Ib) revealed the same histological profile regarding the light and electron microscopic examination.

**Light microscopic and histomorphometric results**

Kidney sections of group I (stained with H& E) revealed the typical structure of renal corpuscles, PCTs and DCTs. The glomerular tuft of capillaries that made up the corpuscles was encircled by Bowman's capsule which is composed of an exterior parietal layer and an interior visceral layer that are spaced by Bowman's space. The PCTs had narrow lumina and lined by cuboidal cells with ill-defined cell boundaries, dark eosinophilic cytoplasm and vesicular rounded basal nuclei. The DCTs had relatively wider lumina than the PCTs. They were lined by cubical cells with relatively pale eosinophilic cytoplasm and vesicular rounded central nuclei (Figure 1A).

H&E- stained renal sections of group II (HFD) appeared with focal structural changes in the cortical renal tissue. Some corpuscles showed detached folded outer “parietal” layer of Bowman’s capsule with focal adhesion within the capillary tuft. Moreover, many of the PCTs appeared disorganized having dilated lumina with apparently decreased height of their lining epithelium. Some PCTs cells showed deep homogenous acidophilic cytoplasm while others showed vacuolated cytoplasm. Some DCTs appeared dilated with focal loss of the lining epithelial cells. Some tubular cells showed pyknotic nuclei, while others were extruded within the lumina of some renal tubules. Exfoliation of the lining cells was also detected in some tubules (Figures 1 B–D). The lumina of some tubules exhibited homogenous acidophilic material (Figure 1E). Some tubular cells appeared binucleated and the interstitium showed mononuclear cellular infiltration (Figure 1F).

Examined H&E-stained sections of kidneys of group III (HFD and MO) revealed that most of renal cortex seemed comparable to that of group I (control) (Figure 1G). However, few focal changes were still detected in the form of vacuolated renal tubular cells (Figure 1H).

By PAS stain in the control group, the PCTs’ cells appeared with intact apical brush borders. A well-defined basement membrane surrounding each of the glomerular capillaries, the corpuscles and the tubules was detected (Figure 2A). However, in HFD group, the brush borders in some PCTs cells were noticed focally lost. The basement membranes around the glomerular capillaries, as well as the renal corpuscles were apparently thickened while that of some renal tubules appeared disrupted (Figure 2B). Group III sections showed a comparable PAS reaction to that of group I (Figure 2C).

Examined Masson's trichrome stained kidney sections of control group (I) revealed that there were few scattered collagen fibers in between the glomerular blood capillaries, around the renal corpuscles and in the interstitium surrounding the renal tubules (Figure 3A). However, HFD group revealed a significant increase in the collagen fibers as compared to the control group which were deposited around the corpuscles and in the interstitium (Figures 3B,C,Table 2). In group III, a significant decrease in collagen content was noticed as compared to HFD group (Figure 3D,Table 2).

Immunohistochemical stained kidney sections for α-SMA showed a negative reaction in the renal cortical tissue of control group (only detected in the media of the blood vessels) (Figure 4A). In group II (HFD), focal strong positive reaction was noticed in some glomeruli as well as in the interstitium. However, moderate positive reaction was also observed in the cytoplasm of some cells of the kidney tubules in group II (Figures 4 B,C). In group III (HFD and MO), scattered faint positive reaction was noticed in the glomeruli and in the interstitium, while the kidney tubules showed negative reaction (Figure 4D). Moreover, the α -SMA reaction mean area percentage was significantly increased in group II as well as group III in comparison to group I, however, a significant decrease was observed in group III in comparison to group II (Table 2).

**Transmission electron microscopic findings**

By TEM, the kidney sections of the rats from group I (control) revealed that the glomeruli consisted of capillaries lined by fenestrated endothelial cells. Intraglomerular mesangial cells were detected in between glomerular capillaries. They showed irregular nuclei and were surrounded by mesangial matrix (Figure 5A). In group II, intraglomerular mesangial cells were apparently increased in number with apparent increase in the mesangial matrix in comparison to the control group (Figure 5B). Sections of group III (HFD and MO) revealed a comparable ultrastructural profile as that of the control group. Intraglomerular mesangial cells were less frequently observed, and they were surrounded by apparently decreased mesangial matrix as compared to HFD group (Figure 5C).

Podocytes in group I were noticed with their processes extending towards the GBM. The cell body of the podocytes extended primary processes from which the secondary or foot processes arose. Between the foot processes of the podocytes, filtration slits appeared and were closed by diaphragms. Sub-podocytic spaces were observed between podocytes' the cell body and the GBM that appeared with uniform thickness (Figure 6A). Podocytes of group II were noticed with relatively fewer indistinct primary and secondary processes in comparison with group I (control). Focal fusion of the secondary processes of the podocytes was frequently observed. Relative reduction in the sub-podocytic space was also noticed. The GBM showed apparent focal thickening (Figures 6 B,C). Podocytes and GBM in group III were more or less comparable to group I. Relatively more numerous primary and secondary processes were seen extending towards the GBM compared to the HFD group with preservation of the sub-podocytic space (Figure 6D).

The cells of the PCTs from the control group appeared resting on a basement membrane and showed rounded nuclei with prominent nucleoli. Mitochondria were arranged longitudinally in between the basal cell membrane infoldings. The apical membrane appeared with numerous microvilli (Figure 7A). In group II, some lining cells of the PCTs had shrunken indented nuclei, electron lucent vacuoles, multiple electron dense bodies and rested on less distinct basement membrane. The cells also showed disorganized mitochondria which were apparently increased in number and smaller in size in comparison to the control group (Figure 7B). In group III, cells of the PCTs were similar to those of the control group (Figure 7C).

Control group's DCT cells were supported by basement membrane. Their nuclei were spherical, and their mitochondria were distributed longitudinally between the distinct infoldings of the basal cell membrane (Figure 8A). In group II, some DCT cells rested on irregular basement membrane. The cells' nuclei were indented and shrunken with irregularly arranged mitochondria and indistinct basal cell membrane infoldings (Figure 8B). In group III, the DCT cells were comparable to the control group (Figure 8C).

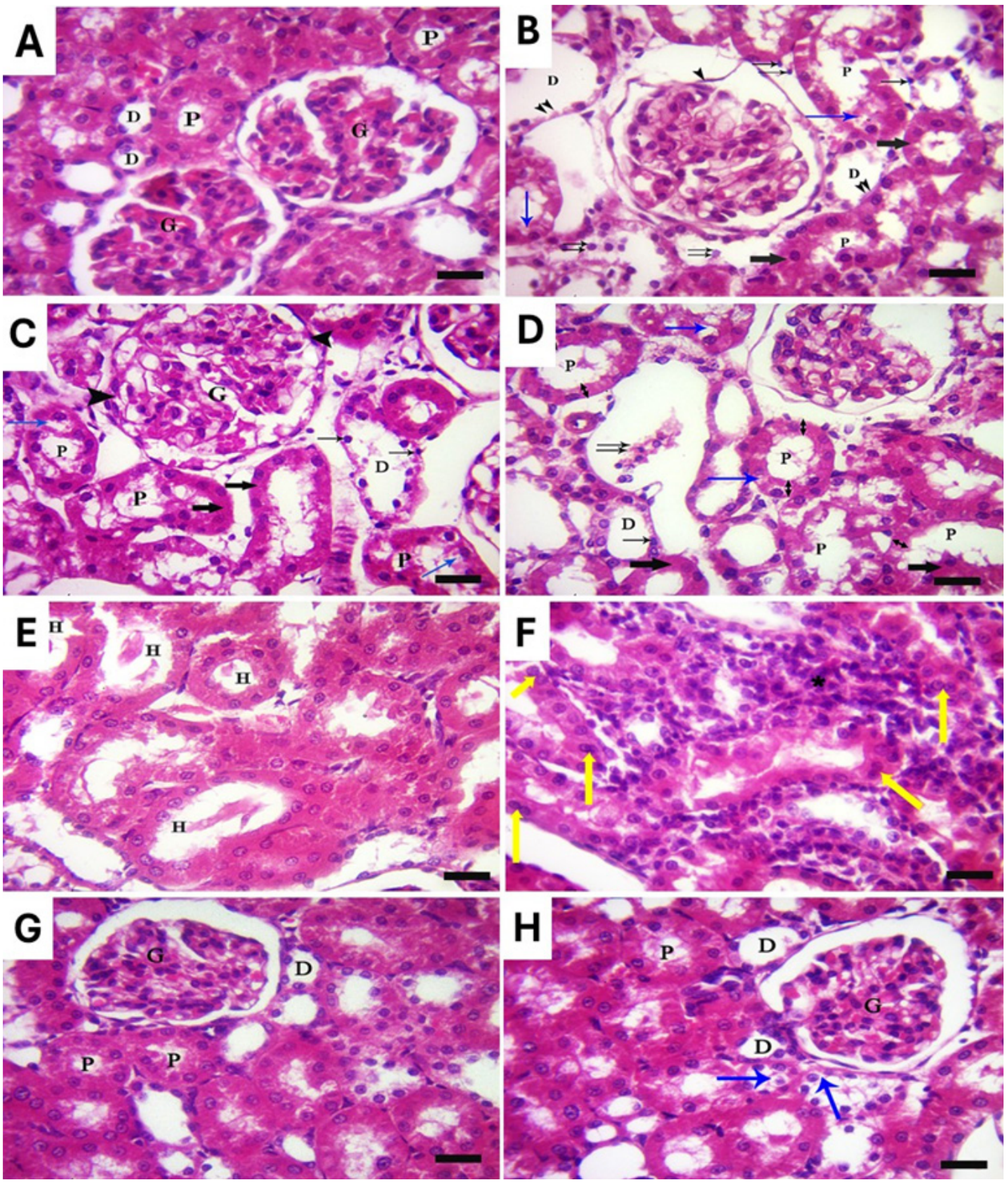


**Fig. 1:** [A] Group I: showing the normal glomeruli, PCTs and DCTs. [B-F] Group II: showing focal adhesions between the glomerular capillaries and Bowman's capsule (▲). Disorganized and dilated PCTs and DCTs having deep homogenous acidophilic cytoplasm (thick arrow) and vacuolated cytoplasm (blue arrow) are seen with focal loss of some tubular cells (▲▲). Some nuclei are pyknotic (↑). Apparent decreased height of PCTs epithelial cells (↕) & exfoliation of tubular epithelial cells (↑↑) are noticed. Homogenous acidophilic material (H) is detected in the lumina of some tubules & Mononuclear cell infiltration (*) in the interstitium. Binucleated tubular cells were noticed (yellow arrow). [G-H] Group III: showing normal structure except focal vacuolated tubular cells (blue arrow). (H &E x400, scale bar=20µm) (G: Glomeruli; P: PCTs; D: DCTs)

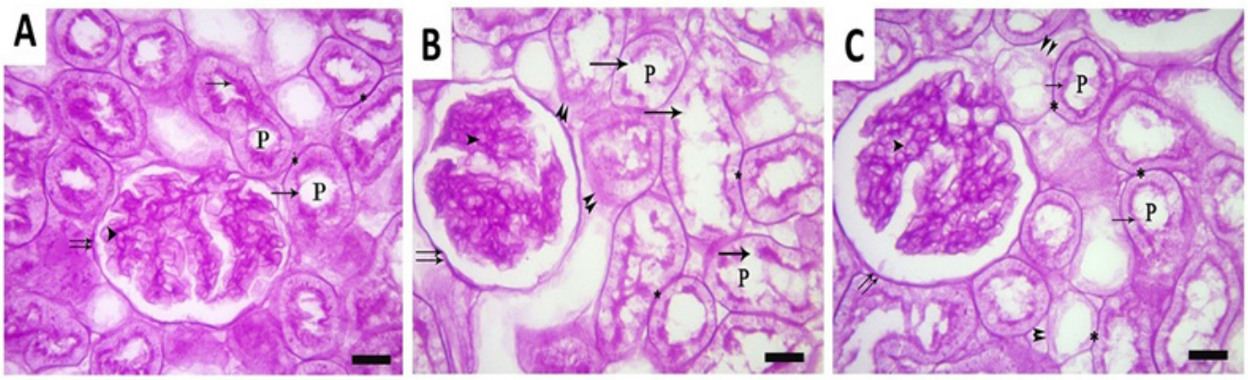


**Fig. 2:** [A] Group I: showing intact PAS positive apical brush borders (↑) of the PCTs cells; well-defined basement membrane of the glomerular capillaries (▲), the renal corpuscle basement membrane (↑↑) and renal tubules basement membrane (*). [B] group II: showing focal isolated loss of apical brush border (↑) of some cells of PCTs; apparently thickened basement membranes of the glomerular capillaries (▲) and the renal corpuscle (↑↑) and disrupted tubular basement membrane (▲▲). [C] group III: showing a comparable PAS reaction to group I with faint basement membranes surrounding some tubules (▲▲). (PAS x400, scale bar=20µm) (P: PCTs).

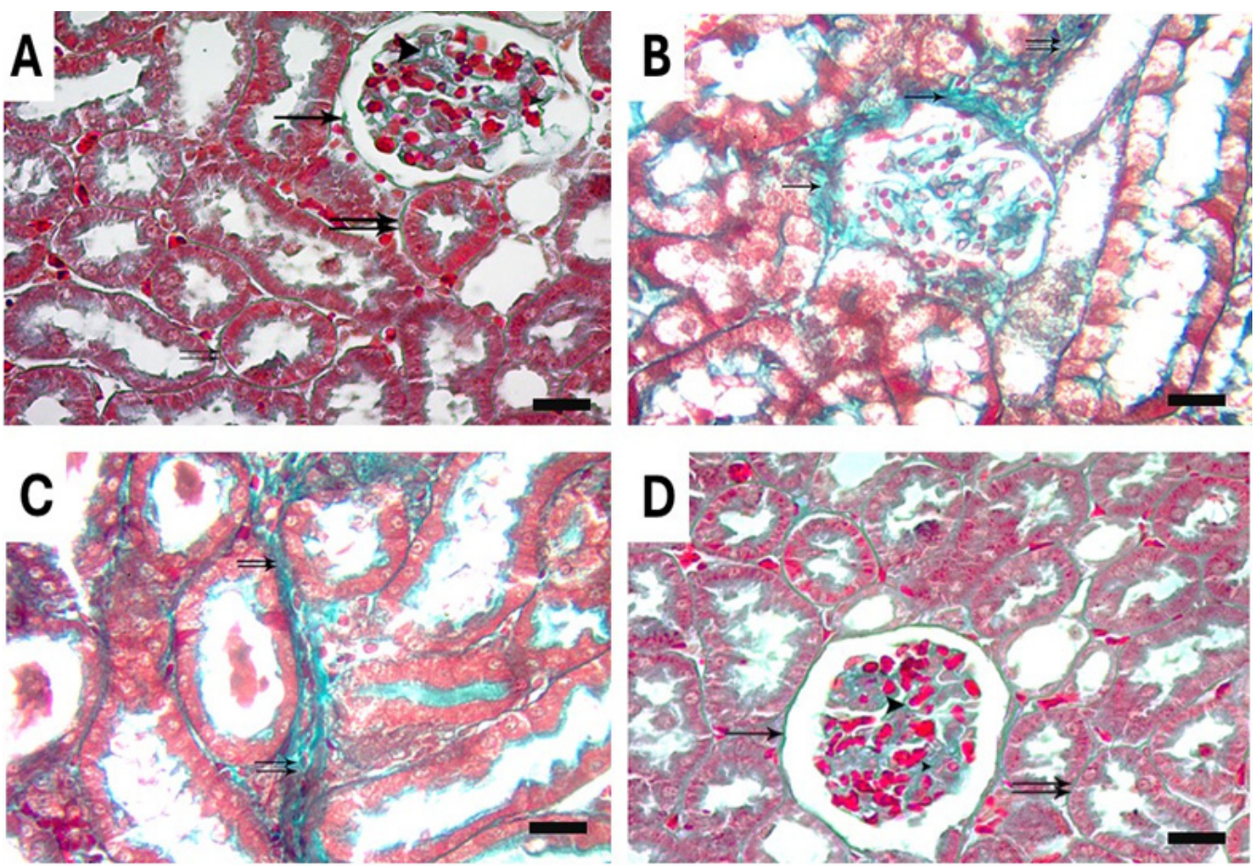


**Fig. 3:** [A] group I: showing scattered few collagen fibers in between glomerular capillaries (▲), around renal corpuscle (↑) as well as in the interstitium (↑↑). [B and C] group II: showing apparent increased collagen fibers around the glomerulus (↑) and in the interstitium (↑↑). [D] group III: showing few scattered collagen fibers in the cortex comparable to group I. (Masson's trichrome x400, scale bar=20µm).

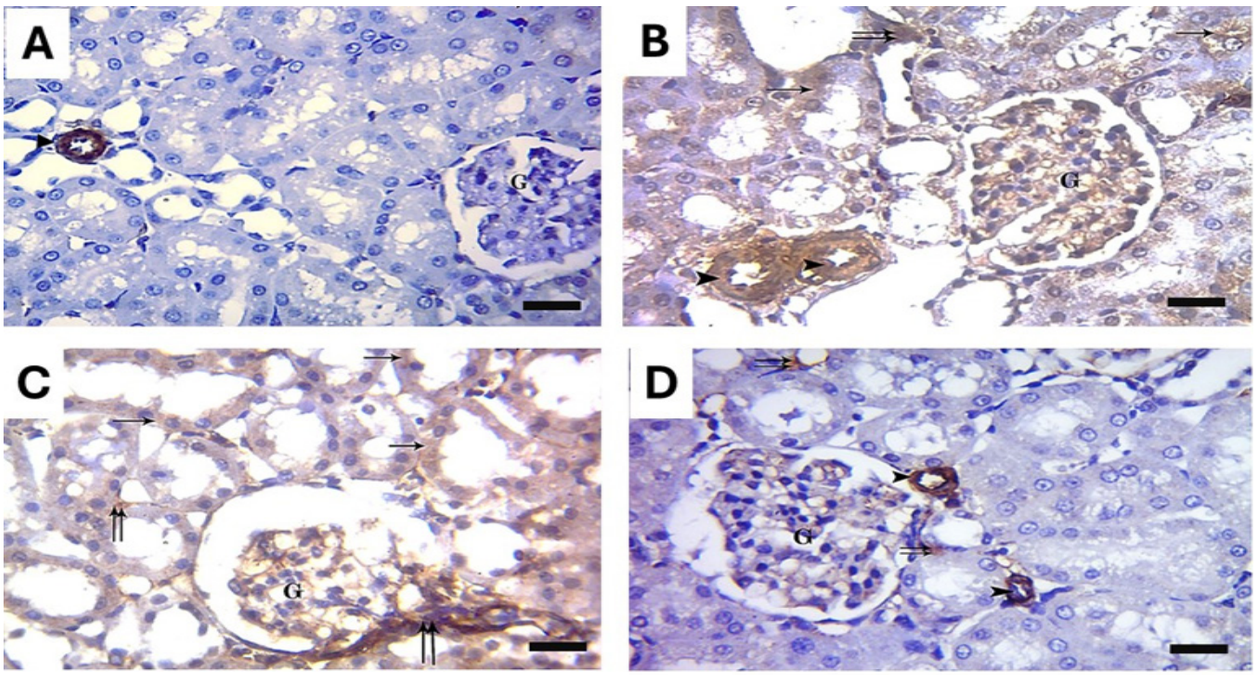


**Fig.4:** [A] group I: showing strong positive cytoplasmic immunoreaction for α-SMA in the smooth muscle cells of the media of the blood vessels (▲). [B and C] group II: showing focal strong positive immunoreaction in the media of blood vessel (▲), the glomerului (G) and the interstitium (↑↑). Some renal tubular cells (↑) show moderate positive immunoreaction. [D] group III: strong positive immunoreaction in the media of the blood vessels (▲). The glomerulus (G) and the interstitium (↑↑) show scattered faint positive immunoreaction, while the renal tubules show negative immunoreaction. (Avidin Biotin Peroxidase technique for α-SMA x400, scale bar=20µm).

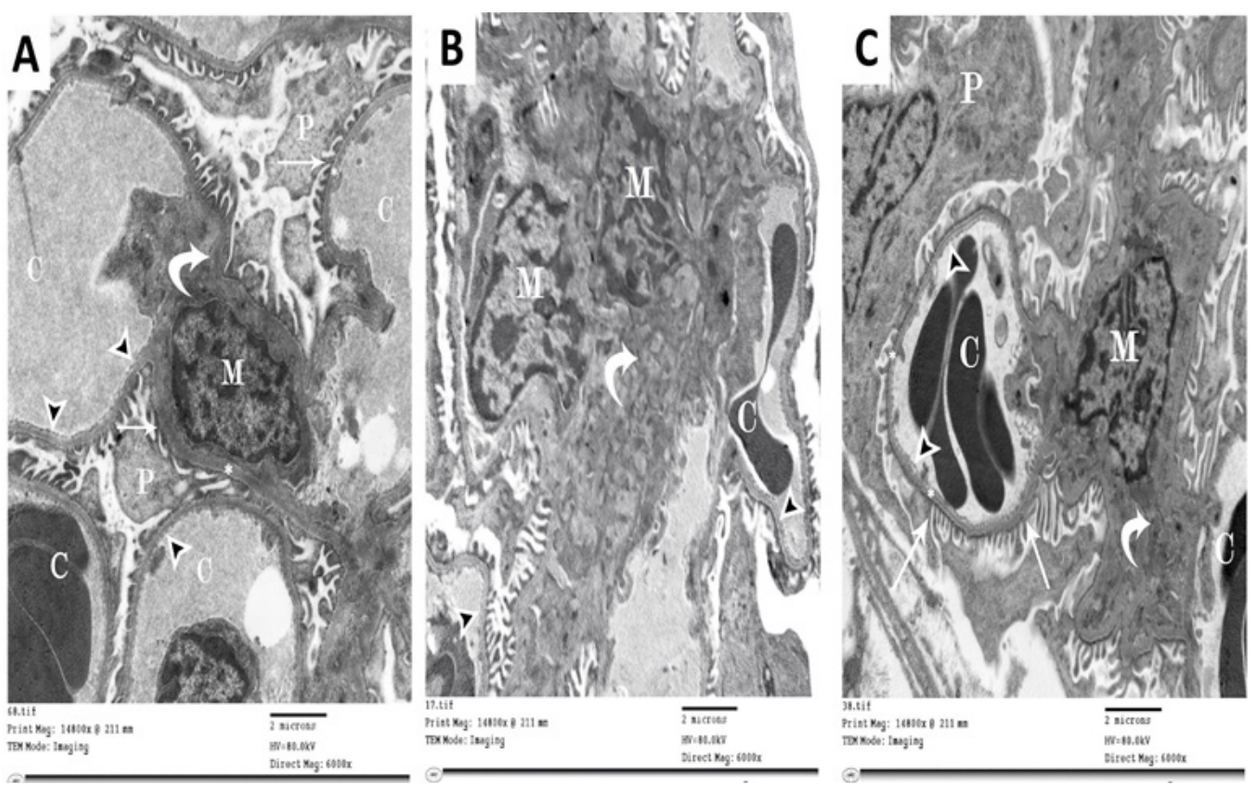


**Fig. 5:** [A] group I: showing that glomerular capillaries are lined by fenestrated endothelium (▲); Intraglomerular mesangial cell with its irregular nucleus is present in between glomerular capillaries and surrounded by mesangial matrix (curved arrow). Podocytes are noticed with their processes (↑) extending towards the GBM (*). [B] group II: showing apparent increase in number of intraglomerular mesangial cells with apparent increase in the surrounding mesangial matrix. [C] group III: showing a comparable structure to group I. (TEM x6000) (C: glomerular capillaries; M: mesangial cell; P: podocytes).

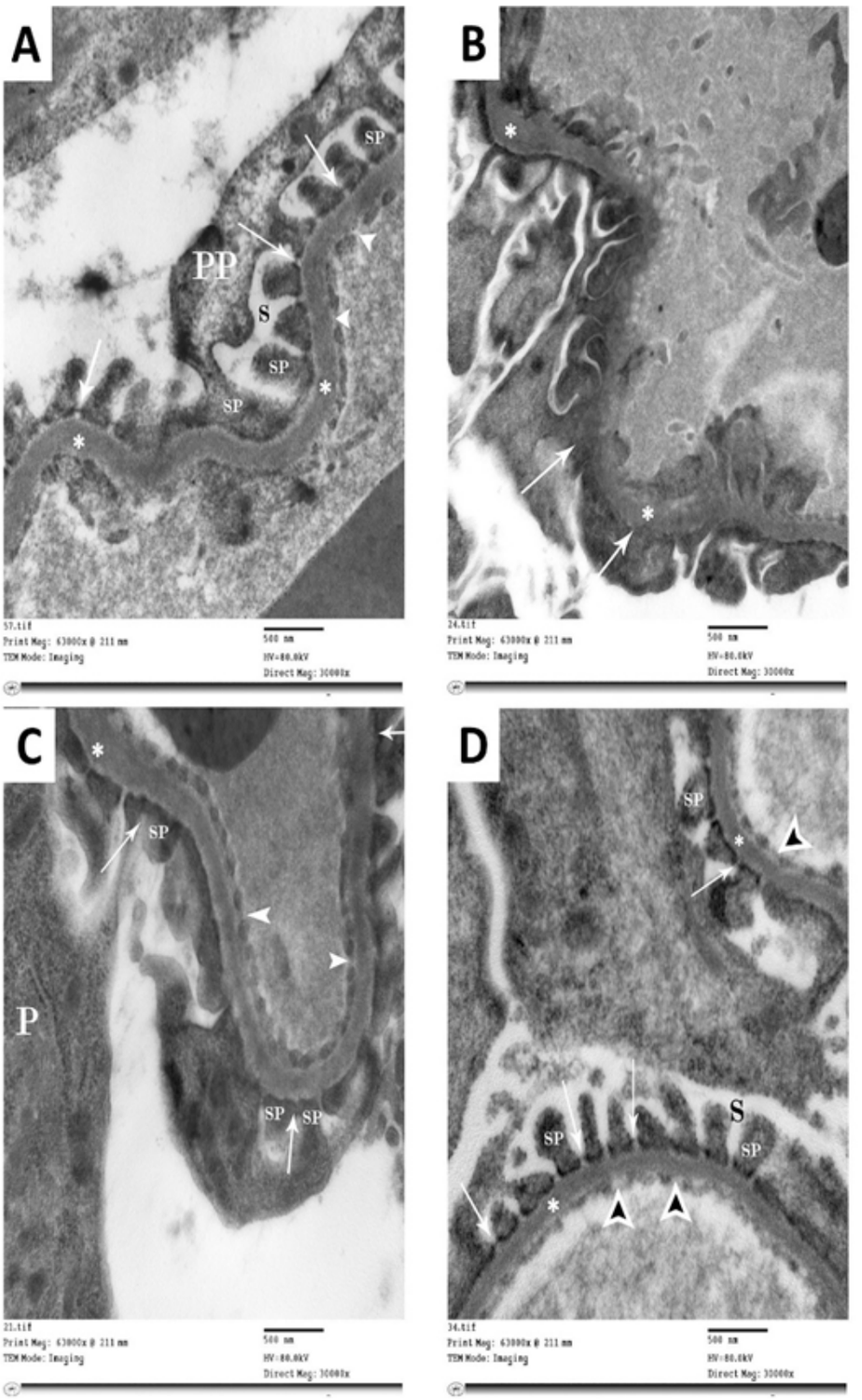


**Fig. 6:** [A] group I: showing a podocyte's primary process separated from the GBM by a sub-podocytic space (S). Filtration slit diaphragms (↑) spanning the slits between secondary processes. The GBM (*) appears uniform in thickness. The endothelium of the glomerular blood capillaries contains fenestrae (▲) not closed by diaphragms. [B and C] group II: showing focal thickening of the GBM (*) and fusion of the secondary processes (↑). Notice the apparent Reduction of the sub-podocytic space. [D] group III: showing comparable structure to group I (TEM x30000) (PP: primary process; SP: secondary process; GBM: glomerular basement membrane; S: sub-podocytic space).

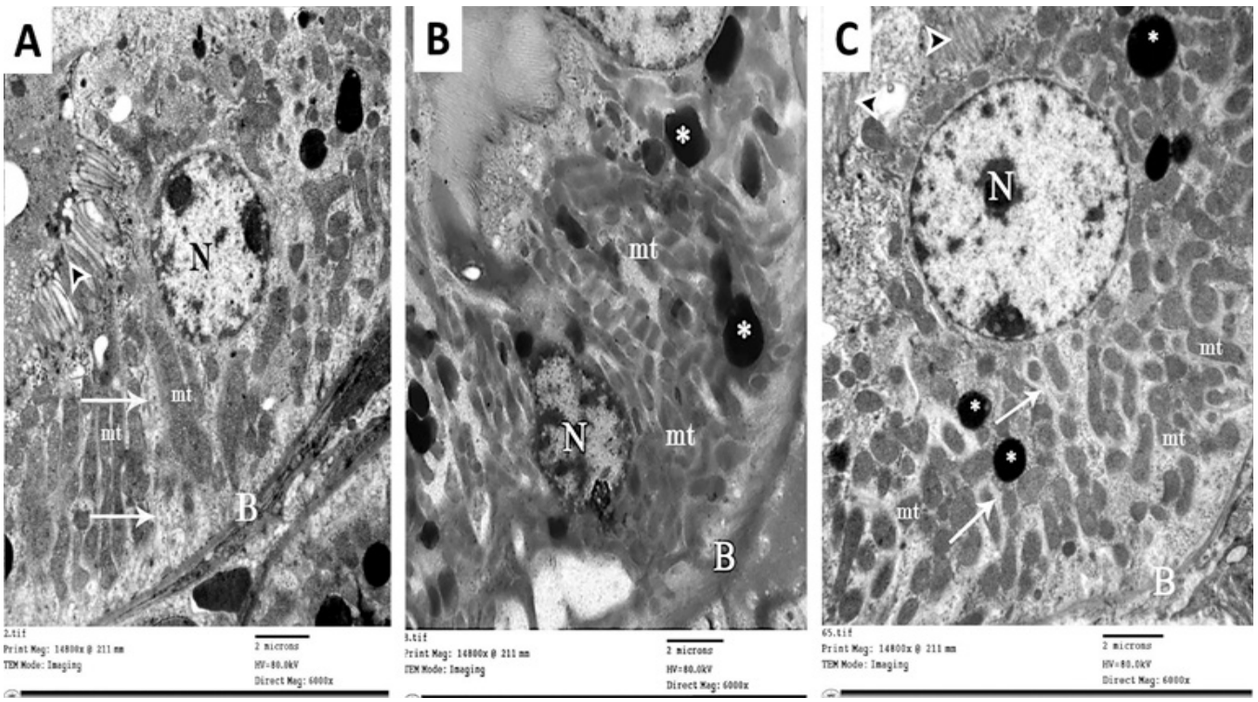


**Fig. 7:** [A] group I: showing a PCT cell resting on a basement membrane, a rounded nucleus with two prominent nucleoli, numerous longitudinally arranged mitochondria in between basal cell membrane infoldings (↑) and apical numerous microvilli (▲). [B] group II: showing a cell of PCT rests on less distinct basement membrane having a shrunken nucleus, multiple electron dense bodies (*) and disorganized mitochondria which are apparently increased in number and smaller in size. [C] group III: showing a cell of PCT with comparable structure to that of group I with multiple electron dense bodies (*). (TEMx6000) (N: nucleus; B: basement membrane; mt: mitochondria).

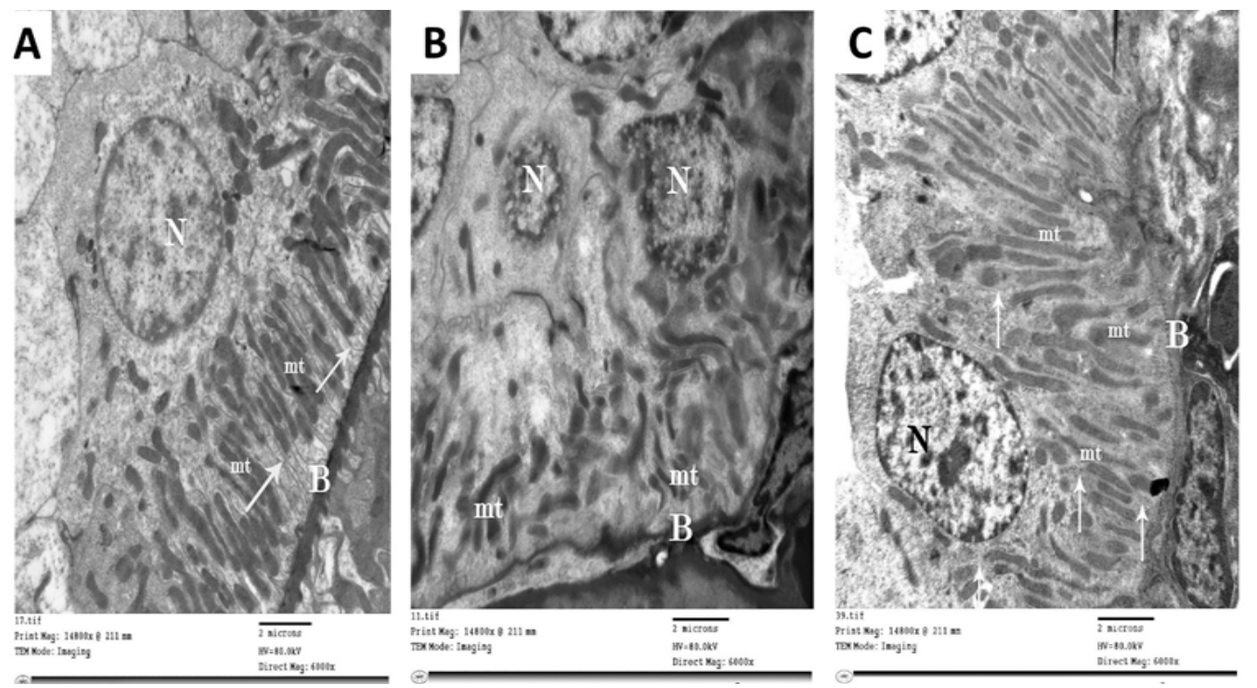


**Fig. 8:** [A] group I: showing a cell of a DCT resting on a basement membrane, spherical nucleus and longitudinally arranged mitochondria in between distinct basal cell membrane infoldings (↑). [B] group II: cells of DCT rests on an irregular basement membrane having shrunken nuclei and irregularly arranged mitochondria with indistinct basal cell membrane infoldings. [C] group III: showing cells of DCT with comparable structure to that of group I (TEM x6000) (N: nucleus; B: basement membrane; mt: mitochondria).

**Table 1:** The mean (± standard deviation) body weight, levels of fasting blood glucose, TG, CH, LDL, HDL, urea, and creatinine of all groups at the end of the experiment

| Parameter | Group I (Control) | | Group II (HFD) | Group III (HFD and MO) |
|---|---|---|---|---|
| | Ia | Ib | | |
| Body weight (gm) | 243.20 ± 9.52 | 245.10 ± 8.95 | 305.80 ± 16.62* | 235.20 ± 10.28^ |
| Fasting blood glucose level (mg/dl) | 86.40 ± 13.97 | 83.70 ± 10.75 | 152.00 ± 23.23 * | 91.20 ± 14.41^ |
| Blood TG Level (mg/dl) | 95.80 ± 19.80 | 100.25 ± 17.65 | 156.20 ± 14.09* | 103.60 ± 11.78^ |
| Blood CH Level (mg/dl) | 105.60 ± 8.26 | 100.83 ± 9.50 | 160.2 ± 13.66* | 99.40 ± 4.82^ |
| Blood LDL Level (mg/dl) | 28.10 ± 2.59 | 27.91 ± 1.86 | 45.14 ± 5.12* | 30.32 ± 2.57^ |
| Blood HDL Level (mg/dl) | 22.48 ± 2.24 | 24.10 ± 1.33 | 16.96 ± 1.31* | 21.40 ± 1.38^ |
| Blood Urea Level (mg/dl) | 37.20 ± 1.99 | 39.01 ±1.68 | 65.47 ± 6.14* | 53.35 ± 4.08*^ |
| Blood Creatinine Level (mg/dl) | 0.61 ± 0.045 | 0.63 ± 0.60 ± .039 | 0.84 ± 0.048* | 0.65 ±.039^ |

TG: triglycerides, CH: cholesterol, LDL: low density lipoprotein, HDL: high density lipoprotein.

Significance: $P<0.05$ * Significant change compared to control group. ^Significant change compared to group II

**Table 2:** Showing the mean area % (± standard deviation) of collagen fibers and α-SMA immune reaction

| Group | Mean area % of collagen fibers± SD | Mean area % of α-SMA ± SD |
|---|---|---|
| Ia | 5.20 ± 0.87 | 2.04 ±.60 |
| Ib | 4.93 ± 1.05 | 1.89 ± 0.75 |
| II (HFD) | 15.70 ± 2.41* | 14.16 ± 2.98* |
| III (HFD and MO) | 6.48 ± 1.68^ | 6.14 ± 1.6*^ |

Significance: $P<0.05$ SD: standard deviation * Significant increase compared to control group. ^Significant decrease compared to group II

## DISCUSSION

Chronic nutrient overload, especially HFD, has been considered as a leading cause of obesity and metabolic syndrome[11]. Moringa oleifera (MO) is a popular herb that has been widely used for multiple purposes such as a dietary supplement, anti-inflammatory and anti-obesity[12].

The current study was conducted to evaluate MO's potential protective effect against the harmful effects of HFD on adult male rats' renal cortex.

The mean body weight of the rats of group II in this study increased significantly in comparison to the control group. Othman *et al*.,2019 explained that HFD creates a condition of positive energy balance leading to increased visceral fat deposition, resulting in weight gain[13]. In comparison to group II, the rats' mean body weight significantly decreased when MO was added to their HFD (group III). It was reported that numerous bioactive chemical components with anti-obesity potential have been found in MO. Of these compounds are cinnamic acid[14] ferulic acid[15] and kaempferol[16].

In the current study, group II (HFD) biochemical data showed a significant decrease in mean blood HDL levels and a significant increase in mean fasting blood glucose, TG, CH, and LDL levels when compared to the control group. These results aligned with the findings of Othman *et al*., (2019). They explained that HFD causes insulin resistance which is characterized by impaired insulin actions in target tissues and reduced glucose uptake by fat and muscle tissues causing hyperglycemia[13]. Furthermore, El-Shehawi *et al*., (2021) added that in HFD- fed obese rats, hyperglycemia and dyslipidemia were due to the development of both leptin and insulin resistance[17].

The biochemical profile of group III was found to be significantly protected by the concurrent administration of MO with HFD. The results of the current investigation showed that the mean blood HDL level significantly increased while the fasting blood glucose, TG, CH, and LDL levels significantly decreased in comparison to group II (HFD). These results were consistent with the work of Ezzat *et al*.,2020 who investigated the ameliorative impact of the ethanolic extract of MO in HFD fed rats[18]. They explained that MO exhibits antioxidant potentials and phenolic components that caused glucose-lowering and hypolipidemic effects. One of the major lipids lowering phenols which they identified in MO extract was quercetin-O-rhamnosyl-hexosyl. Additionally, they reported that the liver's fatty acid synthase and HMG-CoA reductase mRNA expression were suppressed[18].

Regarding the kidney function tests, the mean blood levels of creatinine and urea in group II (HFD) were significantly higher than in the control group. This could be correlated with the structural changes detected by light and electron microscopy in the renal cortex. Similarly, Shams Eldeen *et al*., (2018) detected altered renal function tests in their study on female rats feeding on HFD and their pups[19]. The renal function tests in group III (HFD and MO) of the current study significantly improved as compared to group II. These results were consistent with those of He *et al*. (2022) and Thongrung *et al*. (2023), who investigated

the preventive effect of MO in streptozotocin-induced diabetic rats[20,21]. They attributed this to MO's antioxidant, anti-fibrotic, and anti-inflammatory properties.

Light microscopy examination of the renal cortex of the rats in group II (HFD) in this study showed structural changes, such as glomerular changes, tubular degenerative changes that primarily affected PCTs, as well as mononuclear cellular infiltration. The glomeruli showed localized adhesions between Bowman's capsule and the capillary tuft in HFD (group II). According to Kriz *et al*., (2023) in diabetic nephropathy, local mesangial matrix accumulations caused capillaries to displace peripherally, which allowed podocytes to come in contact with the parietal epithelium and create tuft adhesions to Bowman's capsule[22].

In the lumina of some kidney tubules of group II (HFD), homogenous acidophilic material and sloughed epithelium were observed. This was consistent with the study of Bin-Meferij *et al*., (2019) who reported that the renal tubules' lumen included fragments of necrotic debris and degenerated tubular cells that were sloughed off as hyaline casts[23]. Moreover, Frazier (2019), reported that the intraluminal hyaline casts could be a mixture of cellular debris and proteins precipitated by leakage in the tubular lumina[24].

Moreover, there were multiple dilated renal tubules in group II (HFD). This could be a consequence of the lost brush border of some PCTs together with the decreased height of tubular cells as well as the sloughed epithelium. Some researchers reported that the sloughed tubular epithelium and cast formation following renal injury could block urine flow, resulting in increased intra-tubular pressure with subsequent dilatation of the renal tubules (Abd El Zaher *et al*., 2017)[25].

In addition, some tubular cells in group II (HFD) showed pyknotic nuclei. Going with this finding, Sun *et al*., (2020) noticed threefold increases in tubular cell apoptosis in HFD-fed mice by TUNEL immunostaining. They reported that HFD feeding promoted cytochrome C release from mitochondria into the cytoplasm. They added that the expression of p53 (an upregulated modulator of apoptosis), as well as caspase-3 were highly stimulated suggesting that cytochrome C release activated the proapoptotic pathway[26].

On the other hand, some tubular cells of group II (HFD) showed binucleation. Recently, De Chiara *et al*., (2022) stated that differentiated renal tubular cells lack the capacity to regenerate, but with frequent exposure to complex kidney injury, tubular cells could enter the cell cycle again which is frequently not followed by cell division, and this causes polyploidization. They added that polyploidization allows differentiated tubular cells to maintain residual kidney function during kidney injury[27].

The renal interstitium of group II (HFD) in the current study showed mononuclear cellular infiltration. According to Madduma Hewage *et al*. (2020), PCTs accumulated excessive amounts of saturated fatty acids as a result of HFD. This leads to inflammatory damage since it could trigger the NF-kB inflammatory signaling system to become activated and produce pro-inflammatory cytokines and adhesion molecules[28].

Sections of the renal cortex of group II (HFD) stained with PAS revealed a localized loss of the apical brush borders of some PCTs' cells. According to Ha et al. (2022), this result was caused by oxidative stress, inflammation, and mitochondrial malfunction in the kidneys of mice fed high-fat diet[29]. Adding to that, Liu *et al*., (2023) reported that the expression of Netrin-1, a glycoprotein with a significant renal protection, was reduced in injured kidney triggering actin cytoskeleton derangement which could explain the focal loss of brush border[30]. Moreover, an apparent increased thickness of the basement membranes around glomerular capillaries was also noticed in HFD group by PAS stain. It has been reported that podocytes secrete matrix metalloproteinases, which are linked to extracellular matrix (ECM) remodeling, and type IV collagen and fibronectin, which are the main components of GBM. In response to the profibrotic and inflammatory pathways, the GBM thickens due to reduced turnover and matrix overproduction (Naylor *et al*., 2021)[31].

Rats in group II (HFD) had significantly higher mean area percentages of collagen fibers in their renal cortex than that of rats in group I as shown in examined kidney sections stained with Masson's trichrome. Additionally, Abdollahi et al. (2022) showed that the kidneys of mice given HFD expressed higher levels of transforming growth factor-β1 causing increased collagen deposition[32].

In the renal cortical tissue of group II (HFD), immunohistochemical staining for α-SMA revealed a significant rise in the immune reaction mean area percentage, which was found in the cytoplasm of certain tubular epithelial cells, the interstitium, and some glomeruli. Yuan *et al*., (2019) explained that renal injury leads to transformation of fibroblasts to myofibroblasts (the main producer of fibrotic ECM), and this is enhanced by the production of inflammatory cytokines such as TGF-β[33]. The development of renal interstitial fibrosis was also linked by Sheng and Zhuang (2020) to the epithelial mesenchymal transition (EMT)[34]. They stated that renal tubular cells are crucial to EMT, which is regarded as one of the key mechanisms causing interstitial fibrosis. Apical-basal polarity and cell-to-cell adhesions are lost by the epithelial cells throughout the EMT process, while mesenchymal markers like vimentin and α-SMA are acquired[34].

By TEM examination, group II (HFD) showed an apparently increased number of mesangial cells and mesangial matrix. Recently, Yin et al., (2020) reported that elevated blood glucose level could lead to marked mesangial cells proliferation and ECM expansion due to activation of TGF-β1/SMAD signaling pathway in diabetic rats[35]. So,

mesangial expansion could be correlated to HFD induced hyperglycemia as detected by the biochemical results.

Furthermore, in group II (HFD) the podocytes showed apparently fewer processes with effacement and fusion of the secondary processes. This was accompanied by an apparent decrease in the filtration slit number and width as well as relative reduction of the sub-podocytic space. In view of this point, Sun *et al*., (2020) reported that Nephrin (a junctional protein) was reduced in HFD fed mice leading to effacement of foot processes, actin rearrangement and slit diaphragm breakdown[26].

The focal thickening of the GBM detected in group II (HFD) by PAS was also observed by TEM. Marshall, (2016) explained that podocytes are known to produce GBM components and secrete matrix degrading proteases. However, their injury results in reduced proteases expression, thus playing a main role in GBM thickness alteration[36].

The cytoplasm of PCTs cells of group II (HFD) contained multiple electron lucent vacuoles. Similarly, Szeto *et al*., (2016) noticed filling of the cytoplasm of PCTs in HFD fed mice with many lipid vacuoles. In their trial to get rid of excess lipid accumulation, the PCTs` cells showed increased electron dense bodies which were mostly lysosomes[37]. Additionally, compared to the control group, PCT cells appeared to have more mitochondria. Under HFD diet, Sun et al. (2020) observed that renal tubular cells in mice exhibited continuous mitochondrial fission in response to oxidative stress[26].

Moreover, TEM examination of some cells of DCTs of group II (HFD) showed irregular shrunken nuclei and irregularly arranged mitochondria. Moreover, the basement membrane of some DCTs and PCTs appeared irregular. Bin-Meferij *et al*., (2019) attributed these tubular findings to the HFD associated inflammation and oxidative stress where HFD fed rats showed marked increase in TNF-α and decrease in antioxidants[23].

In the current study, concurrent administration of MO with HFD (group III) was found to exert significant protective effects on the renal cortex. Preservation of the structure and ultrastructure of the kidney cortex was observed except for minor residual effects of the HFD. Glomeruli had an almost normal ultrastructure as regards the mesangium, podocytes` processes, filtration slits, sub-podocytic space and the thickness of the GBM. Furthermore, the majority of the tubules exhibited a structure that was almost normal and comparable to that of the control group. On the other hand, some renal tubular epithelial cells were vacuolated.

Moringa oleifera has acquired a lot of interest in recent years for its excellent biological properties. It shows many protective effects against kidney diseases (Akter et al., 2021)[38]. According to Saka *et al*. (2020), Moringa oleifera has antioxidant and free radical scavenging potentials[39]. Othman *et al*., (2019) reported that treatment with MO extract ameliorated the oxidative stress in HFD fed rats by scavenging reactive oxygen species and production of higher activities of superoxide dismutase (SOD) and catalase[13]. Moreover, Putri *et al*., (2023) noticed improvement of overall kidney structure and increase of SOD antioxidant in kidneys of high fat high fructose fed rats. Moringa oleifera also possesses anti-inflammatory properties[40]. According to Omodanisi *et al*. (2017), MO caused the kidneys of diabetic Wistar rats to reduce production of the inflammatory cytokines, including IL6, TNF-α, as well as monocyte chemoattractant protein-1[41].

In comparison to group II (HFD), the TEM examination of group III (HFD and MO) in the current study showed an apparent decrease in the number of intraglomerular mesangial cells and mesangial matrix. This was in accordance with the results of Wen *et al*. (2022), who found that MO seed extract prevents human renal mesangial cells from proliferating in *vitro* which induced elevated glucose levels[42].

Comparing kidney sections from groups III (HFD and MO) stained with Masson's Trichrome, the mean area percentage of collagen fiber content was significantly lower than that of group II. Park and Chang (2012) previously demonstrated that the administration of MO extract decreased the kidney's TGF-β-induced production of type I collagen and fibronectin[43]. Later, Thongrung *et al*., (2023) reported that in addition to the reduced TGF-β expression, downregulation of collagen type IV genes was also detected in kidneys of streptozotocin diabetic rats treated with MO leaves extract[21].

Additionally, compared to group II (HFD), the mean area percentage of α-SMA was significantly lower in group III (HFD and MO) renal sections that were immunohistochemically stained. According to He *et al*. (2022), MO seeds reduced the expression of TGF-β1, p-SMAD2/3, and α-SMA in streptozotocin-induced diabetic mice and improved tubulointerstitial fibrosis[20].

## CONCLUSION

From the preceding results, it could be concluded that HFD led to a significant increase in the mean weight of the body of the animals as well as significant alterations in the biochemical profile and kidney function tests. In addition, apparent alteration in the light and electron microscopic structure and interstitial fibrosis were observed in the kidney cortex of the rats of group II (HFD).

Concurrent administration of MO with the HFD had an ameliorative and protective effect with a significant reduction of the mean body weight as well as significant improvement of the biochemical parameters. The structural and ultrastructural profile of the kidney cortical tissue of the rats of groups III was similar to the structure and ultrastructural of the control group with few residual affected areas.

In conclusion, the protective effect of MO was prominent as detected by biochemical, microscopic, morphometric and statistical studies.

## RECOMMENDATIONS

Further investigations have to be exerted to discover the potential correlation between the increasing consumption of HFD and the rising incidence of obesity, nephropathy and the metabolic disorders. Confirmatory studies with longer follow up and studying further histological parameters to confirm the effective role of MO.

## CONFLICT OF INTERESTS

There are no conflicts of interest.

## REFERENCES


1. Krisanits, B., Randise, J. F., Burton, C. E., Findlay, V. J., & Turner, D. P. (2020). Pubertal mammary development as a "susceptibility window" for breast cancer disparity. Cancer Health Equity Research, 57–82. doi.org/10.1016/bs.acr.2020.01.004
2. Tang, C., Wang, Y., Xu, Z., Chen, D., Xu, J., Yang, D., Zhan, L., Liu, J., & Kan, J. (2024). The relationships between high-fat diet and metabolic syndrome: Potential mechanisms. Food Bioscience, 59, 104261. doi.org/10.1016/j.fbio.2024.104261
3. McCracken, E., Monaghan, M., & Sreenivasan, S. (2018). Pathophysiology of the metabolic syndrome. Clinics in dermatology, 36(1), 14–20. doi.org/10.1016/j.clindermatol.2017.09.004
4. Guo, Y., Cui, L., Ye, P., Li, J., Wu, S., & Luo, Y. (2018). Change of kidney function is associated with all-cause mortality and cardiovascular diseases: results from the Kailuan study. Journal of American Heart Assoc.;7(21): e010596. doi.org/10.1161/JAHA.118.010596
5. Zhang, X., & Lerman, L. O. (2017). The metabolic syndrome and chronic kidney disease. Translational research: the journal of laboratory and clinical medicine, 183, 14–25. doi.org/10.1016/j.trsl.2016.12.004
6. Gopalakrishnan, L., Doriya, K., & Kumar, D. S. (2016): Moringa oleifera: A review on nutritive importance and its medicinal application. Food Science and Human Wellness, 5(2):49–56. doi.org/10.1016/j.fshw.2016.04.001
7. Bhattacharya, A., Tiwari, P., Sahu, P. K., & Kumar, S. (2018). A Review of the Phytochemical and Pharmacological Characteristics of Moringa oleifera. Journal of pharmacy & bioallied sciences, 10(4), 181–191. doi.org/10.4103/jpbs.jpbs_126_18
8. Assal, Y., Saleh, N., elKafoury, B., Hassan, G., Saleh, H., Hassan ElSayed, M. (2022). Effects of The Anti-glucagon Treatment (Amylin) on Isolated Hearts Performance in Experimentally Induced Type II Diabetes in Rats', Bulletin of Egyptian Society for Physiological Sciences, 42(3), pp. 265-293. doi: 10.21608/besps.2022.121958.1120.
9. Al-Gebily, M.A., Morsy, F.A., El-zawahry, E.I., Ibrahim, D.F., & Abdel-Wahhab, K.G. (2019). Obesity Modulating Efficiency of Moringa oleifera Extract on Obese Modeled Rats. Egyptian Academic Journal of Biological Sciences. C, Physiology and Molecular Biology.11, PP 75-91. doi.org/10.21608/eajbsc.2019.28305
10. Suvarna, K.S., Layton, C. & Bancroft, J.D. (2019). Bancroft's theory and practice of histological techniques. Eighth edition. Churchill Livingstone. ElSevier. doi.org/10.1016/C2015-0-00143-5
11. Wang, L., Wang, H., Zhang, B., Popkin, B. M., & Du, S. (2020-a). Elevated Fat Intake Increases Body Weight and the Risk of Overweight and Obesity among Chinese Adults: 1991-2015 Trends. Nutrients, 12(11), 3272. doi.org/10.3390/nu12113272
12. Pareek, A., Pant, M., Gupta, M. M., Kashania, P., Ratan, Y., Jain, V., Pareek, A., & Chuturgoon, A. A. (2023). Moringa oleifera: An Updated Comprehensive Review of Its Pharmacological Activities, Ethnomedicinal, Phytopharmaceutical Formulation, Clinical, Phytochemical, and Toxicological Aspects. International journal of molecular sciences, 24(3), 2098. doi.org/10.3390/ijms24032098
13. Othman, A.I., Amer, M.A., Basos, A.S., & El-Missiry, M. A. (2019). Moringa oleifera leaf extract ameliorated high-fat diet-induced obesity, oxidative stress and disrupted metabolic hormones. Clinical Phytoscience 5, 48. doi.org/10.1186/s40816-019-0140-0
14. Mnafgui, K., Derbali, A., Sayadi, S., Gharsallah, N., Elfeki, A., & Allouche, N. (2015). Anti-obesity and cardioprotective effects of cinnamic acid in high fat diet- induced obese rats. Journal of food science and technology, 52(7), 4369–4377. doi.org/10.1007/s13197-014-1488-2
15. de Melo, T. S., Lima, P. R., Carvalho, K. M., Fontenele, T. M., Solon, F. R., Tomé, A. R., de Lemos, T. L., da Cruz Fonseca, S. G., Santos, F. A., Rao, V. S., & de Queiroz, M. G. (2017). Ferulic acid lowers body weight and visceral fat accumulation via modulation of enzymatic, hormonal and inflammatory changes in a mouse model of high-fat diet-induced obesity. Brazilian journal of medical and biological research, 50(1), e5630. doi: 10.1590/1414-431X20165630
16. Wang, T., Wu, Q., & Zhao, T. (2020-b). Preventive Effects of Kaempferol on High-Fat Diet-Induced Obesity Complications in C57BL/6 Mice. BioMed research international, 4532482. doi.org/10.1155/2020/4532482
17. El-Shehawi, A. M., Alkafafy, M., El-Shazly, S., Sayed, S., Farouk, S., Alotaibi, S., Madkour, D. A., Khalifa, H. K., & Ahmed, M.M. (2021). Moringa oleifera Leaves Ethanolic Extract Ameliorates High Fat Diet-Induced Obesity in Rats. Journal of King Saud University - Science. 33(6). 101552. doi.org/10.1016/j.jksus.2021.101552

18. Ezzat, S. M., El Bishbishy, M. H., Aborehab, N. M., Salama, M. M., Hasheesh, A., Motaal, A. A., Rashad, H., & Metwally, F. M. (2020). Upregulation of MC4R and PPAR-α expression mediates the anti-obesity activity of Moringa oleifera Lam. in high-fat diet-induced obesity in rats. Journal of ethnopharmacology, 251, 112541. doi.org/10.1016/j.jep.2020.112541

19. Shams eldeen, A. M., Ali Eshra, M., Ahmed Rashed, L., Fathy Amer, M., Elham Fares, A., & Samir Kamar, S. (2018). Omega-3 attenuates high fat diet-induced kidney injury of female rats and renal programming of their offsprings. Archives of physiology and biochemistry, 125(4), 367–377. doi.org/10.1080/13813455.2018.1471511

20. He, B., Wang, X., Zhang, Y., Gao, C., Wu, C., Guo, S., Gu, Y., Li, Q., & Wang, J. (2022). Antioxidant, anti-inflammatory, and anti-fibrotic effects of Moringa oleifera seeds on renal injury diabetic induced by streptozotocin. Journal of Functional Foods. 95,105168. doi.org/10.1016/j.jff.2022.105168

21. Thongrung, R., Pannangpetch, P., Senggunprai, L., Sangkhamanon, S., Boonloh, K., & Tangsucharit, P. (2023). Moringa oleifera leaf extract ameliorates early stages of diabetic nephropathy in streptozotocin-induced diabetic rats. Journal of Applied Pharmaceutical Science,13(08):158–166. doi.org/10.7324/JAPS.2023.89429

22. Kriz, W., Löwen, J., & Gröne, H. J. (2023). The complex pathology of diabetic nephropathy in humans. Nephrology, dialysis, transplantation: official publication of the European Dialysis and Transplant Association - European Renal Association, 38(10), 2109–2119. doi.org/10.1093/ndt/gfad052

23. Bin-Meferij, M.M., El-Kott, A.F., Shati, A.A., &Eid, R. (2019). Ginger extract ameliorates renal damage in high fat diet-induced obesity in rats: biochemical and ultrastructural study. International Journal of Morphology, 37 (2) (2019), pp. 438-447. doi.org/10.4067/S0717-95022019000200438

24. Frazier, K.S. (2019). Pathology of the Urinary System. In: Steinbach, T., Patrick, D., Cosenza, M. (eds) Toxicologic Pathology for Non-Pathologists. Humana, New York, NY. doi.org/10.1007/978-1-4939-9777-0_6

25. Abd El Zaher, F., El Shawarby, A., Hammouda, G., &Bahaa, N. (2017). Role of mesenchymal stem cells versus their conditioned medium on cisplatin-induced acute kidney injury in albino rat. A histological and immunohistochemical study. Egyptian Journal of Histology.; 40(1):37-51. doi.org/10.21608/EJH.2017.3695

26. Sun, Y., Ge, X., Li, X., He, J., Wei, X., Du, J., Sun, J., Li, X., Xun, Z., Liu, W., Zhang, H., Wang, Z. Y., & Li, Y. C. (2020). High-fat diet promotes renal injury by inducing oxidative stress and mitochondrial dysfunction. Cell death & disease, 11(10), 914. doi.org/10.1038/s41419-020-03122-4

27. De Chiara, L., & Romagnani, P. (2022). Polyploid tubular cells and chronic kidney disease. Kidney international, 102(5), 959–961. doi.org/10.1016/j.kint.2022.08.017

28. Madduma Hewage, S., Prashar, S., Debnath, S. C., O, K., & Siow, Y. L. (2020). Inhibition of Inflammatory Cytokine Expression Prevents High-Fat Diet-Induced Kidney Injury: Role of Lingonberry Supplementation. Frontiers in medicine, 7, 80. doi.org/10.3389/fmed.2020.00080

29. Ha, S., Yang, Y., Kim, B. M., Kim, J., Son, M., Kim, D., Yu, H. S., Im, D. S., Chung, H. Y., & Chung, K. W. (2022). Activation of PAR2 promotes high-fat diet-induced renal injury by inducing oxidative stress and inflammation. Biochimica et biophysica acta. Molecular basis of disease, 1868(10), 166474. doi.org/10.1016/j.bbadis.2022.166474

30. Liu, C., Hu, X., Zhao, Y., Huang, A., Chen, J., Lu, T., Wu, M., & Lu, H. (2023). High-Glucose-Induced Injury to Proximal Tubules of the Renal System Is Alleviated by Netrin-1 Suppression of Akt/mTOR. Journal of diabetes research, 2023, 4193309. doi.org/10.1155/2023/4193309

31. Naylor, R. W., Morais, M. R. P. T., & Lennon, R. (2021). Complexities of the glomerular basement membrane. Nature reviews. Nephrology, 17(2), 112–127. doi.org/10.1038/s41581-020-0329-y

32. Abdollahi, M., Kato, M., Lanting, L., Wang, M., Tunduguru, R., & Natarajan, R. (2022). Role of miR-379 in high-fat diet-induced kidney injury and dysfunction. American journal of physiology. Renal physiology, 323(6), F686–F699. doi.org/10.1152/ajprenal.00213.2022

33. Yuan, Q., Tan, R. J., & Liu, Y. (2019). Myofibroblast in Kidney Fibrosis: Origin, Activation, and Regulation. Advances in experimental medicine and biology, 1165, 253–283. doi.org/10.1007/978-981-13-8871-2_12

34. Sheng, L., & Zhuang, S. (2020). New Insights Into the Role and Mechanism of Partial Epithelial-Mesenchymal Transition in Kidney Fibrosis. Frontiers in physiology, 11, 569322. doi.org/10.3389/fphys.2020.569322

35. Yin, J., Wang, K., Zhu, X., Lu, G., Jin, D., Qiu, J., & Zhou, F. (2022). Procyanidin B2 suppresses hyperglycemia-induced renal mesangial cell dysfunction by modulating CAV-1-dependent signaling. Experimental and therapeutic medicine, 24(2), 496. doi.org/10.3892/etm.2022.11423

36. Marshall C. B. (2016). Rethinking glomerular basement membrane thickening in diabetic nephropathy: adaptive or pathogenic? American journal of physiology. Renal physiology, 311(5), F831–F843. doi.org/10.1152/ajprenal.00313.2016

37. Szeto, H. H., Liu, S., Soong, Y., Alam, N., Prusky, G. T., & Seshan, S. V. (2016). Protection of mitochondria prevents high-fat diet-induced glomerulopathy and proximal tubular injury. Kidney international, 90(5), 997–1011. doi.org/10.1016/j.kint.2016.06.013

38. Akter, T., Rahman, M. A., Moni, A., Apu, M. A. I., Fariha, A., Hannan, M. A., & Uddin, M. J. (2021). Prospects for Protective Potential of Moringa oleifera against Kidney Diseases. Plants (Basel, Switzerland), 10(12), 28180. doi.org/10.3390/plants10122818

39. Saka, W. A., Ayoade, T. E., Akhigbe, T. M., & Akhigbe, R. E. (2020). Moringa oleifera seed oil partially abrogates 2,3-dichlorovinyl dimethyl phosphate (Dichlorvos)-induced cardiac injury in rats: evidence for the role of oxidative stress. Journal of basic and clinical physiology and pharmacology, 32(3), 237–246. doi.org/10.1515/jbcpp-2019-0313

40. Putri, I. S., Siwi, G. N., Budiani, D. R., & Rezkita, B. E. (2023). Protective effect of moringa seed extract on kidney damage in rats fed a high-fat and high-fructose diet. Journal of Taibah University Medical Sciences, 18(6), 1545–1552. doi.org/10.1016/j.jtumed.2023.07.001

41. Omodanisi, E. I., Aboua, Y. G., Chegou, N. N., & Oguntibeju, O. O. (2017). Hepatoprotective, Antihyperlipidemic, and Anti-inflammatory Activity of Moringa oleifera in Diabetic-induced Damage in Male Wistar Rats. Pharmacognosy research, 9(2), 182–187. doi.org/10.4103/0974-8490.204651

42. Wen, Y., Liu, Y., Huang, Q., Liu, R., Liu, J., Zhang, F., Liu, S., & Jiang, Y. (2022). Moringa oleifera Lam. seed extract protects kidney function in rats with diabetic nephropathy by increasing GSK-3β activity and activating the Nrf2/HO-1 pathway. Phytomedicine: international journal of phytotherapy and phytopharmacology, 95, 153856. doi.org/10.1016/j.phymed.2021.153856

43. Park, S., & Chang, Y. (2012). Anti-Fibrotic Effects by Moringa Root Extract in Rat Kidney Fibroblast. Journal of Life Science, 22, 1371-1377. doi.org/10.5352/JLS.2012.22.10.1371

**الملخص العربى**

# الدور الوقائي المحتمل للمورينجا أوليفيرا على تأثير النظام الغذائى عالي الدهون على القشرة الكلوية لذكور الجرذان البالغة. دراسة هستولوجية وكيميائية حيوية

**أسماء عبد العزيز إسماعيل عبد العزيز، حنان علاء الدين صالح، جيهان عبد الخالق إبراهيم، فايقة حسن الابيارى**

**قسم علم الانسجة، كلية الطب، جامعة عين شمس**

**المقدمة:** ان استهلاك الغذاء عالى الدهون شائع عالميا ويسبب العديد من المشكلات الصحية مثل امراض الكلى المزمنة. وقد عرف عشب المورينجا اوليفيرا جيدا باستخدامه الواسع لاشتماله على العديد من الخصائص الدوائية.
**الهدف من البحث:** كان الهدف من هذه الدراسة هو تقييم الدور الوقائي المحتمل للمورينجا أوليفيرا الدهنية على تأثير النظام الغذائي عالي الدهون على القشرة الكلوية لذكور الجرذان البالغة.
**المواد والطرق:** أجريت التجربة على ثلاثين من ذكور الجرذان البيضاء البالغة من عمر ٨ أسابيع ووزنها ١٨٠-٢٠٠ جرام. تم تقسيم الجرذان عشوائيا إلى ثلاث مجموعات. المجموعة الأولى: الضابطة، المجموعة الثانية: مجموعة الغذاء عالى الدهون، المجموعة الثالثة: مجموعة الغذاء عالى الدهون بالإضافة لمستخلص المورينجا (٣٠٠ مجم/كجم/اليوم). بعد أربع أسابيع تم وزن جميع الجرذان ثم أخذ عينات الدم للكشف عن مستوى السكر الصائم في الدم والدهون الثلاثية والكوليسترول والبروتين الدهني منخفض الكثافة، وعالي الكثافة، واليوريا، والكرياتينين. تم التضحية بالجرذان واستخراج الكلى. تم تحضير عينات الكلى للفحص المجهري (الضوئي والإلكتروني)، وأُجريت دراسات هستوكيميائية مناعية وإحصائية، واجراء تحليل قياسي.
**النتائج:** أظهرت الحيوانات في المجموعة الثانية (مجموعة الغذاء العالي الدهون) زيادة ذات دلالة إحصائية في متوسط وزن الجسم ومتوسط مستوى سكر الدم الصائم، والدهون الثلاثية، والكوليسترول، والبروتين الدهني منخفض الكثافة، واليوريا، والكرياتينين مقارنة بالمجموعة الأولي. أظهر الفحص المجهري تغيرات موضعية في تركيب القشرة الكلوية حيث أظهرت زيادة موضعية في سمك الغشاء القاعدي للكبيبات مع التصاقات موضعية بين حزمة الشعيرات الدموية ومحفظة بومان، زيادة ظاهرية في عدد خلايا مسراق الكبيبة المتواجدة داخل الكبيبات، مع التصاق الزوائد الثانوية بشكل متكرر وقلة مسافة الفضاء تحت الخلايا الرجلاء. أظهرت بعض الأنابيب الكلوية تركيبا غير منظم واحتوت تجاويف بعض الانابيب على مادة محبة للحمض متجانسة وخلايا متقشرة. أظهرت بعض الانابيب الملتفة القريبة فقدان موضعي للفرشاة القمية لخلاياها كما أظهرت زيادة في عدد الميتوكندريا اتى بدت غير مرتبة وصغيرة في الحجم. أظهر النسيج الخلالي تسلل خلايا أحادية النواة وزيادة في ألياف الكولاجين وتفاعل مناعي إيجابي قوي لأكتين العضلات الملساء (الفا). علي الرغم من ذلك أظهرت مقاطع القشرة الكلوية لجرذان المجموعة الثالثة الحفاظ على التركيب النسيجي، كما أظهرت المجموعة تحسن الفحوصات الكيميائية الحيوية المضطربة وانخفاض وزن الجسم الزائد المستحث بالغذاء عالي الدهون.
**الاستنتاج:** مما سبق نستنتج أن استخدام مستخلص المورينجا المصاحب للغذاء العالي الدهون أدي الي انخفاض بوزن الجسم وتحسن الفحوصات الكيميائية الحيوية للجرذان مع الحفاظ على تركيب القشرة الكلوية.